



Hydrogen interaction with gold nanoparticles and clusters supported on different oxides: A FTIR study

Maela Manzoli, Anna Chiorino, Floriana Vindigni, Flora Boccuzzi*

Department of Inorganic, Physical and Materials Chemistry and NIS Centre of Excellence, University of Turin, via P. Giuria 7, 10125 Turin, Italy

ARTICLE INFO

Article history:

Received 28 February 2011

Received in revised form 26 May 2011

Accepted 20 July 2011

Available online 30 August 2011

Keywords:

Hydrogen activation

Au cluster

Au nanoparticle

Gold hydride

Gold hydroxyl

ABSTRACT

Hydrogen activation is a key step in many reactions like hydrogenations and other processes as the reverse water gas shift reaction. Therefore, the comprehension of the mechanism of hydrogen activation would sustain the understanding of the whole reaction mechanism as well as of the role played either by the gold or by the support. FTIR spectroscopy has been employed as a tool in order to improve the actual knowledge on these topics. Hydrogen interaction with the Au/TiO₂ reference catalyst provided by the World Gold Council, containing mainly gold nanoparticles, and with two samples, Au/CeO₂ and Au/ZrO₂, in which gold clusters are present, has been performed. Hydrogen is dissociated at room temperature on the edge and corner sites of both nanoparticles and clusters, independently from the nature of the support. FTIR evidences of the formation of Au–H and Au–OH species are presented for the first time. These species are strongly bonded to Au and compete with CO adsorption. In addition, the spillover of the H atoms takes place on titania, H atoms are ionized to H⁺ and the released electrons populate the conduction band, as testified by a monotonous absorption that grows at increasing contact time and pressure. The species observed in this paper can play a role on the activity and selectivity of gold catalysts in reactions involving hydrogen dissociation.

© 2011 Elsevier B.V. All rights reserved.

1. Introduction

Hydrogen has great potential as an environmentally clean, renewable and high efficient energy carrier. The development of fuel cell technology has focused a considerable research interest to the design of active, stable and poison-resistant catalysts for low temperature water gas shift (WGS) reaction as well as active and highly selective catalysts for CO preferential oxidation (PROX). The discovery of Haruta that ultrafine gold particles supported on reducible oxides exhibit an exceptional activity in CO oxidation at low temperature inspired increased level of interest in catalysis by gold [1]. The catalytic activity of gold has been attributed to various effects such as the presence of low coordinated atoms, electronic confinement, particle shape and support.

It has been extensively reported that supported gold catalysts are highly active in the WGS reaction at low-temperature [2,3] and more recently also in many hydrogenation reactions [4]. Recent investigations have revealed the beneficial application of ceria as support of active catalysts for methanol decomposition [5] and selective hydrogenation of acetylene [6].

Solymosi et al. [7] have just published a study on the decomposition and reforming of ethanol on supported Au catalysts. They

found that the formation of hydrogen and the product distribution depended sensitively on the nature of the support. In particular, the highest rate of hydrogen evolution was observed on Au/CeO₂, that did not show any deactivation, even after 8 h at 623 K.

Hydrogen activation is a crucial step in many reactions such as some among those reported previously. The comprehension of the activation mechanism of this molecule would lead to a significant improvement in understanding the whole reaction mechanism as well as the role played either by the nanodispersed gold or by the support, assisting the design of better catalysts for more efficient processes. However, it is quite difficult to get experimental evidences of the catalytic activity of gold toward hydrogen dissociation and to disentangle size and support effects.

Recently, Bernal et al. [8] observed strong and fast spillover effects of hydrogen to the support of a preoxidized Au/ceria–zirconia catalyst, while these effects were strongly inhibited by CO coadsorption or by reductive pretreatment.

Density functional theory calculations [9] showed that the catalytic activity of gold supported on stoichiometric and reduced titania surfaces in the H₂ dissociation is strongly affected by the presence of low-coordinated Au atoms. In particular, the number of potentially active sites for H₂ dissociation, that are neutral corner or edge gold atoms in low coordination state and not directly bonded to the support, depends on the shape of the cluster, which is influenced by the nature of the support and by the presence of vacancies and defects. It has been shown that the particles with the

* Corresponding author.

E-mail address: flora.boccuzzi@unito.it (F. Boccuzzi).

largest number of active sites are the two layer particles, consisting of at least one bottom layer of gold atoms in contact with the support and inactive, and one top layer, separated from the support, with low coordinated gold atoms on which H_2 is adsorbed and activated. The presence of O_{vac} , produced by a reductive pretreatment, stabilizes these two layer clusters.

Here we will present FTIR spectroscopic evidences of the formation of Au–H and Au–OH species as a consequence of the hydrogen interaction with different gold samples.

The reference Au/TiO₂ catalyst provided by the World Gold Council (WGC) [10] is compared with two samples, Au/CeO₂ and Au/ZrO₂. The gold reference catalyst data sheet reported that this sample exhibits well dispersed gold particles with average diameter of $83.8 \text{ nm} \pm 1.5 \text{ nm}$; on the contrary, both Au/CeO₂ and Au/ZrO₂ are characterised by the presence of gold clusters [11,12]. The last two samples are very effective in the reverse WGS reaction, where the dissociation of the hydrogen molecules is needed.

The role of the amount of highly uncoordinated gold sites present on the clusters dispersed on zirconia and ceria rather than those exposed at the surface of the nanoparticles supported on titania will be discussed. In addition, the possible effect of the (negative) charge of the Au clusters on ceria will be compared with that of the neutral clusters on zirconia and of the nanoparticles on titania. Therefore, the main goal of the paper is to improve the actual knowledge on the role of the size of the gold species and of the nature of the support in hydrogen dissociation by FTIR spectra analysis.

2. Materials and methods

2.1. Materials

The main features of the catalysts here examined are summarised in Table 1. More in detail, the data presented are inherent to the previous characterisation to which the catalysts were undergone and the references have been indicated.

All samples have been prepared by the deposition–precipitation method, while the Au loading is quite different, as well as the surface area obtained by the Brunauer–Hemmet–Teller (BET) method and the Au particles size. The $\text{mol}_{CO}/\text{mol}_{Au}$ ratio is also reported. This parameter allows to compare directly all samples, since it refers to the number of moles of Au in each sample and above all, it gives us a measure of the number of uncoordinated gold sites able to adsorb CO and presumably to dissociate hydrogen. Looking at the data in Table 1, the Au/TiO₂ reference sample, that contains only nanoparticles has the lowest amount of uncoordinated Au sites. On the contrary, Au/ZrO₂, where only Au clusters are present, shows the highest $\text{mol}_{CO}/\text{mol}_{Au}$ ratio. Finally, the Au/CeO₂ catalyst is characterised by an intermediate $\text{mol}_{CO}/\text{mol}_{Au}$ value (0.074), due to the bimodal Au particle size distribution observed in this case. Therefore, the uncoordinated gold sites can be related to the $\text{mol}_{CO}/\text{mol}_{Au}$ ratio.

2.2. Methods

The FTIR spectra were collected on a Perkin-Elmer 1760 spectrometer (equipped with a MCT detector) with the samples in self-supporting pellets introduced in a cell allowing thermal

treatment in controlled atmospheres and spectrum scanning at controlled temperature.

The curves reported in the figures are the spectral differences between the spectrum related to the bare sample and the spectrum of the sample after the inlet of hydrogen (or also CO, as in the case of Au/ZrO₂). As for hydrogen interaction, the spectra were collected at increasing contact times and/or at increasing pressures. The difference spectra, except those reported in Fig. 5, are not normalized in respect to the gold content or to the amount of the uncoordinated gold sites, determined by the amounts of CO ads/Au at 157 K.

All samples have been submitted to an oxidative pretreatment before the spectroscopic experiments. Moreover, Au/CeO₂ and Au/ZrO₂ have also been reduced. A reductive pre-treatment is needed in the case of Au/CeO₂ and Au/ZrO₂ in order to remove the oxygen atoms or molecules adsorbed on the gold clusters after oxidation. These species, in fact, can inhibit the hydrogen dissociation. On the contrary, Au⁰ sites are already exposed at the surface of the reference Au/TiO₂ even after the thermal treatment in oxygen, as a consequence of the bigger size of the metal particles (see Table 1).

More in detail, the oxidative treatment included heating from room temperature (r.t.) to 473 K under outgassing; followed by an inlet of O₂ (20 mbar) and heating up to 673 K; at 673 K the oxygen was changed three times (20 mbar for 10 min each one). After that, the sample was cooled down to r.t. in oxygen and finally outgassed at the same temperature.

As for the Au/ZrO₂ and Au/CeO₂ catalysts, the reductive treatment was carried out (after oxidation) by heating from r.t. up to 423 K in H₂ (10 mbar), keeping that temperature for 10 min.; then the sample was cooled to r.t. under outgassing.

3. Results and discussion

3.1. Hydrogen interaction with gold nanoparticles

The interaction of hydrogen (from 3 to 50 mbar) with the reference Au/TiO₂ sample at room temperature and at increasing contact times (10 min each step) is shown in Fig. 1. The main peculiarities are a broad absorption at $\sim 3380 \text{ cm}^{-1}$ in the OH stretching region, that gradually increases up to 20 min in 10 mbar H₂ (curve d) and then almost does not change in intensity with the pressure and the contact time and a monotonous absorption extending from 3000 down to 1000 cm^{-1} , that on the contrary increases markedly with the contact time. A band at 1620 cm^{-1} , that grows superimposed to the monotonous absorption, is also evident. This band increases with the pressure and the contact time analogously to the band at 3380 cm^{-1} and reaches its maximum intensity (curves d–f).

The different behaviour of the observed features, i.e. of the 3380 and 1620 cm^{-1} and of the monotonous absorption, indicates that they are due to two different phenomena: the first one is due to the formation of hydrogen containing species involving gold sites, that are quickly saturated, while the monotonous absorption, slowly increasing with the contact time, is related to hydrogen atoms that spillover on the support. It must be stressed that both these features are not observed at all by interaction of hydrogen with the bare support, indicating that the presence of gold sites is essential for the hydrogen dissociation.

Table 1
Main physico-chemical properties of the catalysts.

Sample	Refs.	Au content (wt%)	BET surface area (m^2/g)	Au particles average size (nm)	$\text{mol}_{CO}/\text{mol}_{Au}$ (at 157 K)
Au/TiO ₂	[10,11]	1.5	55	3.8 ± 1.5	0.033
Au/ZrO ₂	[12]	0.47	80	<1.5	0.13
Au/CeO ₂	[13]	3.0	118	clusters < 1 nm and particles 10–25 nm	0.074

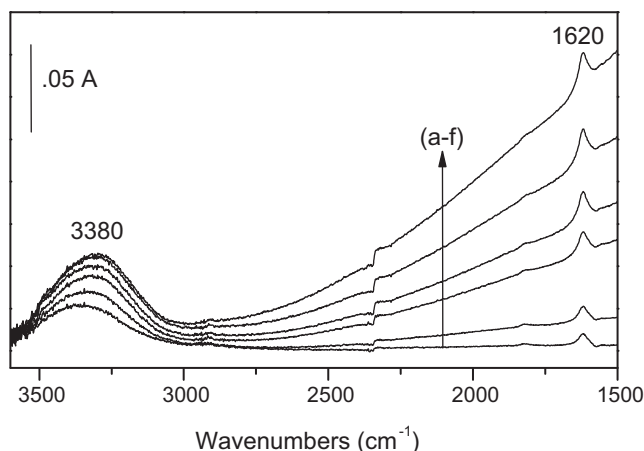


Fig. 1. FTIR difference spectra collected upon admission of 3 mbar of H₂ (curve a), 5 mbar of H₂ (curve b), after 10 min (curve c), after 20 min (curve d), 50 mbar of H₂ (curve e), after 10 min (curve f) on the reference Au/TiO₂ sample at r.t.

More in detail, the band at 3380 cm⁻¹, that is irreversible to the outgassing at r.t. (data not shown for the sake of brevity), appears quite similar to the broad band at 3100–3500 cm⁻¹ detected and assigned to Au–OH hydrogen bonded species [14] over an unsupported gold powder after interaction with hydrogen. At the same time, the band at 1620 cm⁻¹, in spite of its position, is not due to the bending mode of water. Firstly, we found that also this band is not reversible to the outgassing and secondly, in additional experiments involving water interaction with the same sample, we observed the formation of bands in the OH stretching and in the water bending region whose relative intensity and shape are completely different from those of the bands here discussed. Moreover, the bands significantly decrease in intensity upon outgassing at the same temperature. Finally, water adsorption on bare titania produces a spectrum in the OH stretching region with different shape and absorption frequency of the bands, that show intensities significantly larger than that in the water bending region ([2] and references therein).

On these basis, we conclude that hydrogen is dissociated on gold sites giving Au–OH and Au–H species. Therefore, we assign the band at 3380 cm⁻¹ to Au–OH species on gold atoms at the interface with the titania, where the Au atoms of the nanoparticles are in close contact with the oxygen of the support, representing the only possibility to form Au–OH species. We propose here the assignment of the 1620 cm⁻¹ band to the Au–H stretching mode of a hydride adsorbed on the edge or corner sites of the metallic particles. The assignment, that will be more deeply discussed later on, is supported by a similar absorption frequency observed for gold hydrides obtained by reaction of laser-ablated gold atoms from metallic gold with H₂ in cryogenic conditions [19].

As for the monotonous absorption, it is ascribed to population of the titania support conduction band, occurring as a consequence of the ionization of atomic hydrogen, dissociated on gold uncoordinated sites and spilt over on the support. On titania, as reported by Panyatov and Yates [15], H atoms may be ionized to H⁺ by donating an electron into a shallow trap state close to the bottom of the conduction band, thereby making H an n-type dopant. The donated electron enters into a shallow defect state located in the band gap about 0.12 eV below the bottom of the conduction band [15] and, upon thermal excitation, it is excited into the conduction band where it is highly delocalized. Atomic hydrogen is able to induce metallicity in metal/metal oxide systems. The n-doped electronic system can absorb IR radiation over a continuum of IR photon energies, leading to the observed increase in the background absorbance in the IR spectral range (see curves b–f in Fig. 1). The electronic

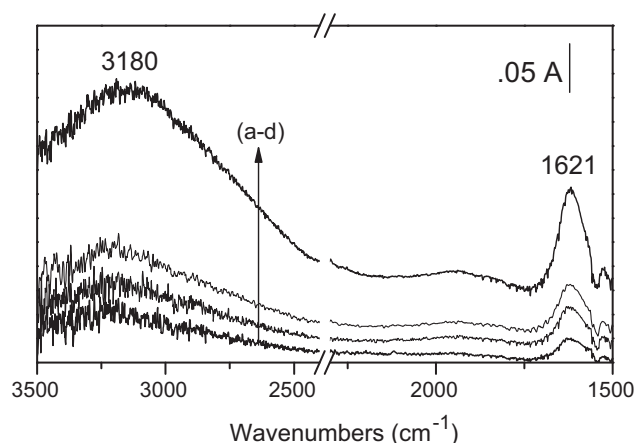


Fig. 2. FTIR difference spectra collected upon admission of 3 mbar of H₂ (curve a), 15 mbar of H₂ (curve b), 50 mbar of H₂ (curve c) and after 3 h (curve d) on the Au/ZrO₂ sample at r.t.

absorption is completely depleted upon interaction with oxygen (data not shown), indicating that the contact with oxygen, adsorbed at the surface of titania as O₂⁻ species, induces a localization of the free electrons produced by the interaction with hydrogen and, consequently the loss of the metallization effect reported in Fig. 1.

3.2. Hydrogen interaction with gold clusters

The FTIR spectra collected on Au/ZrO₂ and Au/CeO₂ upon hydrogen interaction at room temperature are reported in Figs. 2 and 3, respectively. In both cases there is no formation of any monotonous absorption neither increasing pressures nor extending contact times, differently from what happens on the reference Au/TiO₂ catalyst.

The lack of the monotonous electronic absorption (Fig. 2) is expected in the case of the zirconia-supported sample. In fact, as a consequence of the insulator nature of ZrO₂, the hydrogen spilled over cannot induce population of the conduction band.

Surprisingly, also for the Au/CeO₂ sample, there are no changes in the overall IR absorbance (Fig. 3). Ceria is an n-type semiconductor oxide, as titania. The different behaviour of ceria may be understood taking in account that Ce³⁺ ions are formed after the reduction treatment. The electrons are strongly localized in the f orbitals of the Ce³⁺ ions, as testified by the narrow absorption at

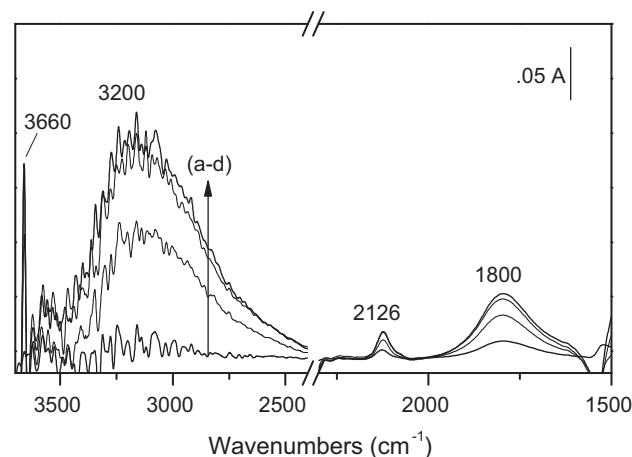


Fig. 3. FTIR difference spectra collected upon admission of 50 mbar of H₂ (curve a), after 10 min (curve b), after 1 h (curve c) and after 3 h (curve d) on the Au/CeO₂ sample at r.t.

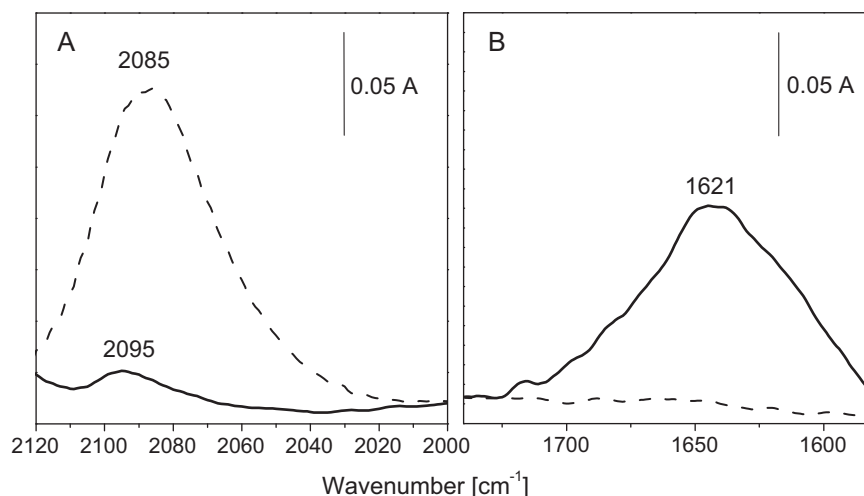


Fig. 4. FTIR difference spectra of 3.5 mbar CO adsorbed at low temperature before (dashed curve) and after (solid curve) hydrogen interaction on Au/ZrO₂ in the carbonylic region (A) and in the Au–H stretching region (B).

2126 cm^{−1}, that increases immediately after the inlet of H₂ and gradually reaches the maximum intensity by increasing the contact time (3 h, curve d). This band has been already observed by some of us on reduced Au/CeO₂ catalysts before CO admission [13] and assigned, according to Daturi et al. [16], to the forbidden $^2F_{5/2} \rightarrow ^2F_{7/2}$ electronic transition of Ce³⁺ located at defective lattice sites. Therefore, the free electron-like absorption is not produced. However, similarly to the depletion of the monotonous absorption observed for Au/TiO₂, the band at 2126 cm^{−1} disappears by contact with oxygen (not shown for sake of brevity). In both cases the depletion is a consequence of the formation of surface O₂[−] species by reaction with the free electrons on Au/TiO₂ and by reaction with the strongly localized f electrons of Ce³⁺ centers on Au/CeO₂.

More in detail, the interaction of hydrogen with Au/ZrO₂ (reported in Fig. 2) produces a broad absorption in the OH stretching region, centered at ~3180 cm^{−1}, that significantly increases with the contact time, and a component at 1621 cm^{−1}, that grows up at the same time. The same interaction of hydrogen with Au/CeO₂ (Fig. 3) produces a band at 3200 cm^{−1} that depends on the contact time (up to 3 h), together with the narrow and strong component at 3660 cm^{−1}, peculiar of the reduced Au/CeO₂ sample, and a component at 1800 cm^{−1}. Both absorptions at 3180–3200 cm^{−1} can be assigned to Au–OH stretching modes.

In the case of Au/CeO₂, a band at 3660 cm^{−1} is observed (Fig. 3). It is assigned to OH groups close to Ce³⁺ ions, generated on ceria surface during the reductive treatment in H₂. These sites are few in number and behave as isolated ones, as evidenced by the shape, very sharp, of the band. The same feature has been already observed at 3670–3650 cm^{−1} on reduced CeO₂ [13,16].

The band at 1621 cm^{−1} observed on Au/ZrO₂ (Fig. 2) could be related either to the formation of a water-like species or to hydride species, Au–H and Zr–H. A FTIR study of hydrogen adsorbed on Ru/ZrO₂ [17] reported spectroscopic features which are in some extent similar to those shown in Fig. 2. The assignment there reported was to a water-like species and it was strongly supported by isotopic exchange with D₂. In those experiments, three bands were detected at 1604, 1411 and 1186 cm^{−1}, indicating the formation of water-like species and excluding the assignment of the band to Ru–H or Zr–H species. We also performed this kind of experiment and observed that, after heating in D₂ up to 423 K, only two bands at 1621 and at 1290 cm^{−1}, rather than three, have been produced (not shown for sake of brevity). Therefore, in our case, the band at 1621 cm^{−1} should be due to an hydride species.

The assignment to Zr–H can be ruled out, as a consequence of the band behaviour to the outgassing: in the present paper it is completely irreversible to the outgassing up to 473 K, while it has been previously reported that bands at 1562 and at 1371 cm^{−1}, due to two different Zr–H species, gradually disappeared by gentle evacuation of hydrogen at r.t. [18].

As for gold hydrides, they have been obtained by reaction of laser-ablated gold atoms with H₂ in cryogenic conditions [19]. The Au–H stretching frequency observed and calculated was in the range of 1636–1642 cm^{−1}, quite close to the one here reported. Therefore, we assign the band at 1621 cm^{−1} to the stretching mode of a Au–H species. Coming back to the band at 1620 cm^{−1} observed on the Au/TiO₂ sample (Fig. 1) we confirm also for this band the assignment to a Au–H species.

The band at 1800 cm^{−1}, detected in the case of Au/CeO₂ (Fig. 3), has been already detected by some of us on the same sample and tentatively assigned to an Au–H vibrational mode [20]. Its frequency is higher than that related to the band found on Au/ZrO₂ and on the reference Au/TiO₂, and also higher than that reported for the Au–H species observed by reaction of laser ablated atoms [19]. This feature is possibly due to an effect on the negative charge of the gold clusters on reduced Au/CeO₂. Gold hydride species have been also extensively studied by theoretical calculations, looking either at the size of gold or at the effect of the charge [21,22]. In particular, in [22] it is shown that an increase of the stretching vibrational frequency is produced going from neutral to negatively charged gold clusters, according to our findings.

3.3. Probing the gold sites after interaction with hydrogen

In order to get additional information on the gold sites able to dissociate the hydrogen molecule, CO adsorption at low temperature before and after hydrogen interaction has been performed. For the sake of brevity, only the results of the experiment performed on Au/ZrO₂ have been reported in Fig. 4.

A symmetric band at 2085 cm^{−1} is produced on the freshly reduced sample after CO adsorption at low temperature (dashed curve in Fig. 4A). This absorption has already been assigned by some of us to carbonylic species on uncoordinated sites of Au clusters [12]. The inlet of CO after interaction with hydrogen reveals a dramatic decrease in intensity of the band at 2085 cm^{−1}, that now is shifted at 2095 cm^{−1}. At the same time, upon interaction with hydrogen, the band at 1621 cm^{−1} related to Au hydride is formed

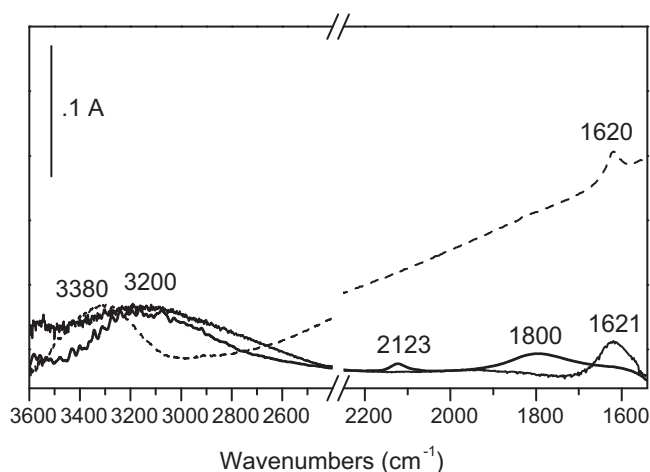


Fig. 5. FTIR difference spectra normalised on the $\text{mol}_{\text{CO}}/\text{mol}_{\text{Au}}$ ratio and collected upon admission of 50 mbar of H_2 at r.t. on the reference Au/TiO₂ sample (dashed curve), on the Au/ZrO₂ sample (fine curve) and on the Au/CeO₂ sample (bold curve).

(Fig. 4B). Fig. 4 well evidences that almost no CO is adsorbed on the Au/ZrO₂ catalyst when the Au–H species is present, indicating that both CO and H₂ compete for the same uncoordinated gold sites: at room temperature the CO probe is not able to take off the H atoms from the Au adsorption sites, indicating, in agreement with the literature [8], that the Au–H bond is strong and energy is needed to break it.

3.4. Correlation of hydrogen dissociation with the amount of gold uncoordinated sites

As already stated in the experimental section the spectra of the hydrogen interaction on the three samples are not normalised. However, as shown in the previous paragraph, a competition between hydrogen and CO has been put in evidence. In Fig. 5 we have tried to compare directly the FTIR difference spectra of the reference Au/TiO₂ sample (dashed curve), the Au/ZrO₂ sample (fine curve) and the Au/CeO₂ sample (bold curve) after maximum contact time with 50 mbar of H₂ at r.t. The spectra are normalised by the parameter $\text{mol}_{\text{CO}}/\text{mol}_{\text{Au}}$ ratio, reported in Table 1, that provides the amount of uncoordinated gold sites able to adsorb CO, referred to the number of moles of Au in each sample (see Table 1).

The comparison shows that the intensities of the bands related both to hydroxyls and hydride species observed on the samples are quite comparable after the normalisation, more similar for Au/CeO₂ and Au/ZrO₂. This finding can be taken as an indication that the uncoordinated Au sites which chemisorb the CO molecule are also involved in the hydrogen dissociation, as evidenced in Fig. 4.

Au/TiO₂ reference sample behaves slightly differently, with a band related to Au–H species that appears weaker. This feature is probably observed with a reduced intensity because the free electron population of the titania conduction band induces “a metal-like reflectivity” of the sample, causing a reduced penetration of the beam and preventing the vibrational bands from being fully revealed; moreover the band concerns only a small amount of the total gold particles. In fact, if considering the size distribution reported in Table 1, the Au–H vibrational mode observed must be related only to the species formed on the very small size fraction of gold particles, while for the particles of bigger size present on this sample (see Table 1), the metallic nature of gold makes inactive the IR mode. This is well known on platinum and on other metals where there are chemisorbed hydrogen species which have not been detected by infrared spectroscopy. If the hydrogen atoms form

bridges between two or three metal atoms, the stretching mode would be expected to give dipole changes parallel to the surface. Taking in account the unique property of metals, that is the freedom of the conduction electrons to respond to an electrical stimulation, an antiparallel dipole change will be also produced at the metal surface: the result will be an overall IR inactive mode, as a consequence of the “metal-surface selection rule” [23].

As for the apparently lower intensity also of the hydroxyl band observed for Au/TiO₂ if compared to the corresponding absorptions observed for Au/CeO₂ and Au/ZrO₂, it can be related to the presence for these last samples of a larger concentration of gold sites in contact with the support as a consequence of the small size of their gold clusters [11,12].

4. Conclusions

Hydrogen molecules are dissociated at room temperature on both gold nanoparticles and clusters, independently from the nature of the support. However, on the three examined samples, the FTIR spectroscopic features are quite different: on gold supported on titania, hydrogen is dissociated on the edge and corner sites of the nanoparticles with size 3.8 ± 1.5 nm. Some H atoms remain adsorbed on the gold metallic sites of the smallest particles and the Au–H species is detected at 1620 cm^{−1}. At the same time, other H atoms are adsorbed on the gold sites in contact with the oxide, producing an absorption due to Au–OH species at 3380 cm^{−1} and some H atoms spilled over the support, where they are ionized as H⁺ and e[−]. Atomic hydrogen spillover is testified by the monotonous absorption that grows with the contact time and the pressure, indicating that the donated electrons populate the shallow donor sites of titania, easily producing almost free electrons.

As for gold on zirconia and on ceria, as a consequence of the presence of small non metallic clusters, with a large amount of gold atoms in contact with the oxidic supports, a quite strong band at 3200 cm^{−1} related to Au–OH species is produced. Moreover, Au–H bands at 1620 and 1800 cm^{−1} are detected. These species are quite strongly bonded and compete with CO for the adsorption on the uncoordinated gold sites.

A relationship between the uncoordinated gold sites present on the samples in different amounts and the formation of the hydroxyl and hydride species has been found: the gold sites able to chemisorb CO are able to dissociate hydrogen, too.

The different species observed and discussed in this paper may play a role on the activity and selectivity of gold catalysts involving the hydrogen molecule.

Acknowledgement

The authors gratefully acknowledge the Istituto Italiano di Tecnologia (IIT) – Project Seed “NANOGOLD” for financial support.

References

- [1] M. Haruta, Catal. Today 36 (1997) 153–166.
- [2] F. Boccuzzi, A. Chiorino, M. Manzoli, D. Andreeva, T. Tabakova, J. Catal. 188 (1999) 176–185.
- [3] D. Andreeva, V. Idakiev, T. Tabakova, A. Andreev, J. Catal. 158 (1996) 354–355.
- [4] L. McEwan, M. Julius, S. Roberts, J.C.Q. Fletcher, Gold Bull. 43 (2010) 298–306, and references therein.
- [5] C. Kartusch, J.A. van Bokhoven, Gold Bull. 42 (34) (2009) 3–348, and references therein.
- [6] A.C. Gluhoi, J.W. Bakker, B.E. Nieuwenhuys, Catal. Today 154 (2010) 13–20.
- [7] A. Gazsi, A. Koós, T. Bãnsági, F. Solymosi, Catal. Today 160 (2011) 70–78.
- [8] S.E. Collins, J.M. Cies, E. Del Rio, M. Lopez-Haro, S. Trasobares, J.J. Calvino, J.M. Pintado, S. Bernal, J. Phys. Chem. C 111 (2007) 14371–14379.
- [9] M. Boronat, F. Illas, A. Corma, J. Phys. Chem. A 113 (2009) 3750–3757.
- [10] Sample number 17C, supplied by World Gold Council, <http://www.gold.org>.
- [11] F. Menegazzo, M. Manzoli, A. Chiorino, F. Boccuzzi, T. Tabakova, M. Signoretto, F. Pinna, N. Pernicone, J. Catal. 237 (2006) 431–434.

- [12] F. Menegazzo, F. Pinna, M. Signoretto, V. Trevisan, F. Boccuzzi, A. Chiorino, M. Manzoli, *Appl. Catal. A: Gen.* 356 (2009) 31–35.
- [13] T. Tabakova, F. Boccuzzi, M. Manzoli, D. Andreeva, *Appl. Catal. A: Gen.* 252 (2003) 385–397.
- [14] E. Quinet, L. Piccolo, H. Daly, F.C. Meunier, F. Morfin, A. Valcarcel, F. Diehl, P. Avenier, V. Caps, J. Rousset, *Catal. Today* 138 (2008) 43–49.
- [15] D.A. Panayotov, J.T. Yates Jr., *J. Phys. Chem. C* 111 (2007) 2959–2964.
- [16] M. Daturi, E. Finocchio, C. Binet, J.C. Lavalley, F. Fally, V. Perrichon, *J. Phys. Chem. B* 103 (1999) 4884–4991.
- [17] H. Ishikawa, J.N. Kondo, K. Domen, *J. Phys. Chem. B* 103 (1999) 3229–3234.
- [18] T. Onishi, H. Abe, K. Maruya, K. Domen, *J. Chem. Soc. Chem. Commun.* 61 (1985) 7–618.
- [19] X. Wang, L. Andrews, *Angew. Chem. Int. Ed.* 42 (2003) 5201–5206.
- [20] T. Tabakova, M. Manzoli, F. Vindigni, V. Idakiev, F. Boccuzzi, *J. Phys. Chem. A* 114 (2010) 3909–3915.
- [21] G.-J. Kang, Z.X. Chen, Z. Li, X. He, *J. Chem. Phys.* 130 (2009) 034701.
- [22] S. Zhao, Y.L. Ren, Y.L. Ren, J.J. Wang, W.P. Yin, *J. Phys. Chem. A* 114 (2010) 4917–4923.
- [23] H.A. Pearce, N. Sheppard, *Surf. Sci.* 59 (1976) 205–217.